

## Theory of a scanning tunneling microscope with a two-protrusion tip

Michael E. Flatté

*Department of Physics and Astronomy, University of Iowa, Iowa City, Iowa 52242*

Jeff M. Byers

*Naval Research Laboratory, Washington, D.C. 20375*

(Received 21 December 1995)

We consider a scanning tunneling microscope (STM) such that tunneling occurs through two atomically sharp protrusions on its tip. When the two protrusions are separated by at least several atomic spacings, the differential conductance of this STM depends on the electronic transport in the sample between the protrusions. Such two-protrusion tips commonly occur during STM tip preparation. We explore possible applications to probing dynamical impurity potentials on a metallic surface and local transport in an anisotropic superconductor.

Scanning tunneling microscopy (STM) enables the characterization of materials on the atomic scale through measurements of the local density of states (LDOS). Recently, in a series of STM experiments on the Cu(111) surface, the local transport properties of electrons in a Shockley surface state were probed through their influence on the LDOS around an Fe impurity.<sup>1</sup> A similar experiment has been proposed for measuring the transport properties of a high-temperature superconductor.<sup>2</sup> These experiments detect the reflection from the impurity of electrons injected by the STM. The spatial resolution of these experiments is sub-Angstrom. Properties which might be determined from these types of measurements, but could not be probed by a STM measurement on the homogeneous sample, include the *angularly resolved* dispersion relations and mean free path, as well as the density of states as a function of energy and momentum. In the Cu experiments the dispersion relation was measured, no evidence for density-of-states anisotropy with angle was found, and the mean free path was too large to detect.

A stronger signal would result from an independent method of injecting electrons at a site (by another contact) and detecting them elsewhere with a STM. The possibilities for this have been explored in recent work<sup>3,4</sup> and will be referred to as the two-contact experiment. A related technique, applicable to transport on a longer length scale ( $\mu\text{m}$ ), uses a laser to create nonequilibrium quasiparticles and a point contact to detect them.<sup>5</sup>

The STM is also sensitive to the spectroscopic properties of impurities.<sup>6,7</sup> However, a STM averages over the fluctuating part of an impurity potential, such as that of a free orbital moment, making it difficult to observe. Such free moments are of great interest, in part because their interaction with conduction electrons may produce a Kondo resonance.

We suggest in this paper an experiment which should provide detailed angular information about fluctuating impurity potentials and probe transport on a homogeneous sample. The apparatus, shown schematically in Fig. 1, would consist of a spatially extended STM tip with two protrusions, each ending in a single atom. Although the case of STM tips with tunneling at more than one place has been considered before,<sup>8</sup> that work was concerned with tips ending in *clusters* with substantial tunneling through more than one atom. The

images obtained from these STM tips tended to be blurry and less useful than those from single-atom-terminated contacts. Here we propose a tip with two atomically sharp protrusions, and will demonstrate that new information is obtainable when these protrusions are separated by more than  $10 \text{ \AA}$ . In contrast to the difficulties associated with arranging two independent *contacts* in close proximity, two-*protrusion* tips are often created by chance during tip preparation, with tip separations up to  $1000 \text{ \AA}$ .<sup>9</sup> The interference between the two protrusions influences tunneling conductances at a lower order in the tunneling matrix elements than the two-contact experiment. The two-protrusion experiment, therefore, should be easier to construct and have greater signal than the two-contact experiment.

For separations of  $10 \text{ \AA} - 100 \text{ \AA}$  a two-protrusion tip would be useful for probing the angular structure of a free moment. The differential conductivity depends on the angle-resolved amplitude for electrons to scatter from the impurity. A measurement with a single-protrusion STM tip merely measures backscattering. For an impurity state *fixed* relative to the lattice orientation by the crystal field, backscattering is sufficient to determine the impurity's angular structure; therefore the single-protrusion measurement provides as much information as the two-protrusion one. However, for identifying the angular structure of a *free* moment, the two-protrusion tip is superior to the single-protrusion tip. A two-contact experiment could in principle measure this angular structure as well,<sup>4</sup> but positioning two tips within  $100 \text{ \AA}$  of

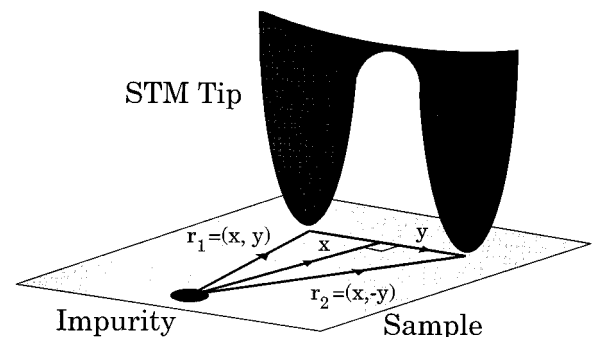


FIG. 1. Probe-sample geometry. Two protrusions on a single STM contact are connected to the same reservoir.

each other would be extremely difficult.

On a homogeneous sample the transport quantities of interest would determine the desired separation of protrusions on the STM tip. Measurements of quantities with long length scales (100 Å–1000 Å) such as mean free paths, transitions from ballistic to diffusive propagation, low- $T_c$  superconductors' coherence lengths, charge-density-wave correlation lengths, and angularly anisotropic density-of-states effects<sup>2</sup> would most benefit from the increased signal of the two-protrusion configuration relative to the two-contact configuration. It is also at these distances that the overlapping interference of other impurities on a surface would complicate a measurement performed with a single-protrusion STM around an impurity. However, for electronic quantities with short length scales, such as Fermi wavelengths, the single-protrusion STM would likely perform the best of the three.

The two-protrusion tip is treated according to a generalization of the Tersoff-Hamann approximations<sup>10</sup> appropriate for the new geometry. Although there are circumstances where more complicated tip models would be appropriate, the Tersoff-Hamann approximations have proved successful for many surfaces.<sup>11</sup> In certain geometries multiple scattering paths from tip to surface can interfere, as has been shown for benzene on rhodium<sup>12</sup> and platinum.<sup>13</sup> Our model calculations are performed for protrusions located at least 10 Å laterally away from an impurity, so electronic paths from tip to impurity to surface, which provide the interesting effects in the benzene work, are strongly suppressed.

The tunneling Hamiltonian

$$H_T = \int d\mathbf{x} d\mathbf{r} [T(\mathbf{x}, \mathbf{r}) \psi^\dagger(\mathbf{x}) \phi(\mathbf{r}) + \text{H.c.}], \quad (1)$$

where  $\psi(\mathbf{x})$  is the field annihilation operator for an electron at position  $\mathbf{x}$  in the STM tip, and  $\phi(\mathbf{r})$  is the field annihilation operator for an electron at position  $\mathbf{r}$  in the sample. The electron spin is treated implicitly to simplify the notation. The differential conductance of the STM at  $T=0$  K,

$$\frac{dI}{dV} = \frac{2e^2}{h} \int d\mathbf{x} d\mathbf{r} d\mathbf{x}' d\mathbf{r}' T(\mathbf{x}, \mathbf{r}) T^*(\mathbf{x}', \mathbf{r}') \times \text{Im}g(\mathbf{x}, \mathbf{x}'; 0) \text{Im}G(\mathbf{r}', \mathbf{r}; eV), \quad (2)$$

where  $G$  is the Green function in the sample and  $g$  is the Green function in the STM tip.

Typically the transfer function  $T(\mathbf{x}, \mathbf{r})$  is taken to be localized near a point in the sample and the tip:  $T(\mathbf{x}, \mathbf{r}) = Wv(\mathbf{x} - \mathbf{x}_0)v'(\mathbf{r} - \mathbf{r}_0)$ , where the integrals of  $|v|^2$  and  $|v'|^2$  are unity. With  $v'$  a highly localized function the differential conductance is proportional to

$$\begin{aligned} \text{Im}\tilde{G}(\mathbf{r}_0, \mathbf{r}_0; eV) &= \text{Im} \int d\mathbf{r} d\mathbf{r}' v'(\mathbf{r} - \mathbf{r}_0) \\ &\quad \times v'(\mathbf{r}' - \mathbf{r}_0) G(\mathbf{r}, \mathbf{r}'; eV) \\ &\sim \text{Im}G(\mathbf{r}_0, \mathbf{r}_0; eV). \end{aligned} \quad (3)$$

When  $v$  is also very localized the proportionality constant is  $e^2|W|^2N(0)/h$ , where  $N(0)$  is the density of states

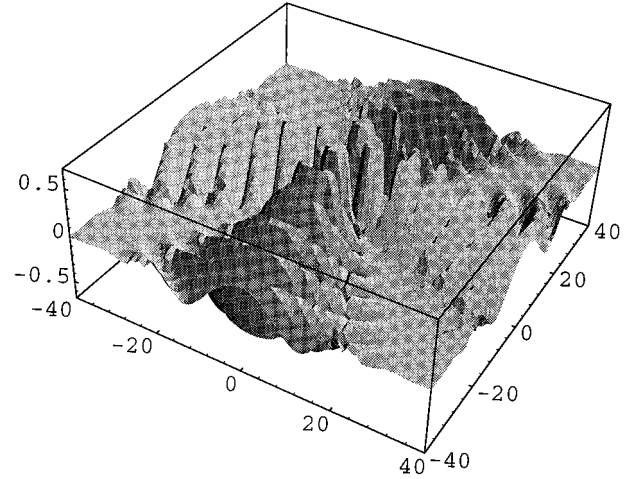


FIG. 2. Single-protrusion STM differential conductance for an impurity  $d$  state with  $\xi = 2k_V^{-1}$  in units of  $e^2|W|^2N(0)N_s/h$ , where  $N(0)$  and  $N_s$  are the tip's and sample's density of states.  $x$  and  $y$  have units of  $k_V^{-1}$ .

in the tip at the Fermi energy. The expression  $dI/dV = e^2|W|^2N(0)\text{Im}G(\mathbf{r}_0, \mathbf{r}_0; eV)/h$  is a common starting point for STM theory.<sup>10</sup>

We model the effect of a single impurity resonance by the Hamiltonian term

$$H_I = \int d\mathbf{r} [A(\mathbf{r}) \phi(\mathbf{r})^\dagger \chi + A^*(\mathbf{r}) \phi(\mathbf{r}) \chi^\dagger], \quad (4)$$

where  $\chi$  is the annihilation operator for an electron in the localized state. For a simple model,<sup>14</sup>  $A(\mathbf{r}) \propto \Psi(\mathbf{r})$ , the (normalized) wave function of the impurity state. The Green function is then

$$\begin{aligned} G(\mathbf{r}_1, \mathbf{r}_2; eV) &= \int d\mathbf{r} d\mathbf{r}' G(\mathbf{r}_1, \mathbf{r}; eV) \frac{A(\mathbf{r})A^*(\mathbf{r}')}{eV - E_I + i\Gamma} \\ &\quad \times G(\mathbf{r}', \mathbf{r}_2; eV) \end{aligned} \quad (5)$$

$$\begin{aligned} &= \int d\mathbf{r} d\mathbf{r}' G(\mathbf{r}_1, \mathbf{r}; eV) \frac{\Psi(\mathbf{r})\Psi^*(\mathbf{r}')}{\pi N_s} \\ &\quad \times G(\mathbf{r}', \mathbf{r}_2; eV), \quad eV = E_I, \end{aligned} \quad (6)$$

where  $E_I$  and  $\Gamma$  are the energy and linewidth of the impurity state and  $N_s$  is the density of states of the sample at  $E_I$ . We assume there is no other influence on  $\Gamma$  besides hopping to the extended states. For a  $d$  state,  $\Psi(\mathbf{r}) = (2/\xi\sqrt{\pi})e^{-r/\xi}\cos(2\theta_r)$ , where  $\xi$  is the range of the state. For a fixed  $d$  state,  $\theta_r$  is measured relative to a crystallographic axis. Figure 2 shows the single-protrusion differential conductance in the vicinity of a fixed impurity  $d$  state with  $\xi = 2k_V^{-1}$  ( $k_V$  is the wave number of the electronic state with energy  $eV$ ). It shows clear fourfold symmetry. If the crystal-field splitting of the impurity levels is larger than the temperature and  $\Gamma$ , the STM can separately probe each nondegenerate level by adjusting the voltage.

The two-protrusion experiment becomes more useful than the single-protrusion experiment when the impurity of interest has a free moment. Then the  $dI/dV$  must be averaged over orientations of  $\theta_r$  in Eq. (6) (and Fig. 2). The two-

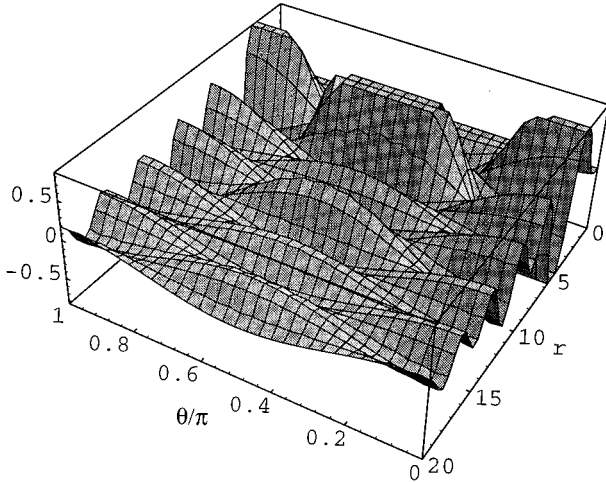


FIG. 3. Two-protrusion STM differential conductance for an impurity  $d$  state in the same units as Fig. 2. The two tips are assumed to be the same distance from the impurity. The differential conductance is plotted as a function of tip-impurity distance  $r$  (units of  $k_V^{-1}$ ) and relative angle  $\theta$ . The two-protrusion STM differential conductance shows clear fourfold angular symmetry. The single-protrusion STM signal corresponds to  $\theta=0$ .

protrusion transfer function, however, contains contributions from both tunneling sites below the protrusions:  $T(\mathbf{x}, \mathbf{r}) = \sum_i W_i v_i(\mathbf{x} - \mathbf{x}_i) v'_i(\mathbf{r} - \mathbf{r}_i)$ , where for simplicity we consider  $v$ ,  $v'$ , and  $W$  to be independent of  $i$ . The STM current for this system is

$$\frac{dI}{dV} = \frac{2e^2 |W|^2}{h} \sum_{\{i,j\}=1}^2 \text{Im} \tilde{g}(\mathbf{x}_i, \mathbf{x}_j; 0) \text{Im} \tilde{G}(\mathbf{r}_j, \mathbf{r}_i; eV). \quad (7)$$

The  $i=j$  terms describe direct tunneling through the two protrusions, but the  $i \neq j$  terms are interference terms between the two protrusions. We approximate  $\text{Im} \tilde{g}(\mathbf{x}, \mathbf{x}'; 0)$  by  $N(0) \exp(-|\mathbf{x} - \mathbf{x}'|/\ell_I)$ , where  $\ell_I$  is the inelastic mean free path.<sup>15</sup> A favorable tip material would have a large  $N(0)$  and a long  $\ell_I$ . Figure 3 shows two-protrusion results for a  $d$  orbital that is free to move in the plane of the surface. The  $dI/dV$  is plotted as a function of distance from the impurity  $r$  (same for both protrusions) and angle  $\theta$  between the two tips. A single-protrusion measurement corresponds to  $\theta=0$ . The fourfold structure of the  $d$  orbital is clearly visible in Fig. 3, which should be thought of as a compilation of results which must come from many different tips.

A result for a particular tip, with separation  $6\pi k_V^{-1}$ , is shown in Fig. 4. The differential conductance through the two protrusions at  $\mathbf{r}_1 = (x, 3\pi)$  and  $\mathbf{r}_2 = (x, -3\pi)$  is compared to the differential conductance of a single protrusion located at  $\mathbf{r}_1$  with tunneling matrix element  $2W$ . The geometry is shown in Fig. 1. Each protrusion is thus at least 10 Å from the impurity during this measurement, ensuring that there are no significant direct tip-impurity interactions. The differential conductances for  $x=0$  ( $\theta=\pi$ ) are identical and at large  $|x|$  (where  $\theta$  is small) the two are very similar. The most prominent difference is the strong suppression of features in the two-protrusion  $dI/dV$  near  $x = \pm 3\pi$ . Since  $\theta = \pi/2$  for  $x = 3\pi$ , the direct  $i=j$  terms are almost fully cancelled by the  $i \neq j$  terms in Eq. (7). As a remarkable fea-

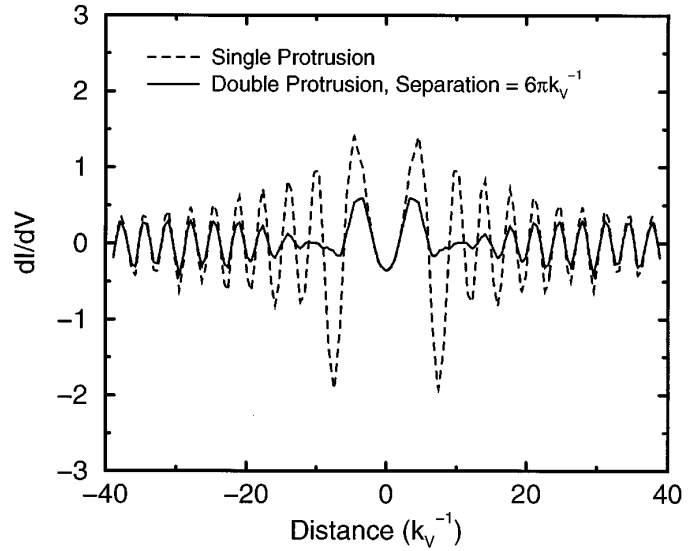


FIG. 4. Comparison of two-protrusion and single-protrusion STM differential conductance for a fixed tip separation of  $6\pi k_V^{-1}$ , where the two protrusions are oriented as shown in Fig. 1.

ture near  $x = 3\pi$ , the oscillations in the two-protrusion  $dI/dV$  increase in magnitude as the distance from the impurity grows.

We emphasize there is no need to rotate the tip assembly to perform this measurement. If the impurity moment is free, for any tip orientation the geometry of Fig. 1 can be arranged solely by translation of the tip. The orientation and protrusion separation of the tip can be identified by analyzing the double image from an impurity or a step edge.

We now apply Eq. (7) to transport between the two protrusions through a  $d_{x^2-y^2}$ -gapped superconductor. A  $d_{x^2-y^2}$  gap has been proposed<sup>16</sup> for high- $T_c$  superconductors, including  $\text{Bi}_2\text{Sr}_2\text{CaCu}_2\text{O}_8$ . A very clean surface can be prepared on  $\text{Bi}_2\text{Sr}_2\text{CaCu}_2\text{O}_8$  so that transport is ballistic, and the mean free path is  $10^3 - 10^4$  Å (Ref. 17) at 4.2 K.

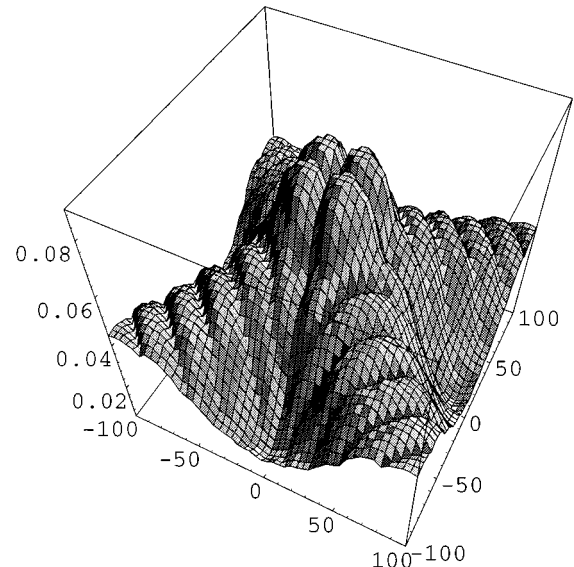


FIG. 5. Differential conductance in position space, same units as Fig. 2. The sample is a superconductor with a  $d_{x^2-y^2}$  gap,  $eV = 0.1\Delta_{\text{max}}$ ,  $\Delta_{\text{max}} = 0.1\epsilon_F$ , and  $k_V \sim 1 \text{ \AA}^{-1}$ . The inelastic mean free path is taken to be  $\ell_I = 500 \text{ \AA}$ .

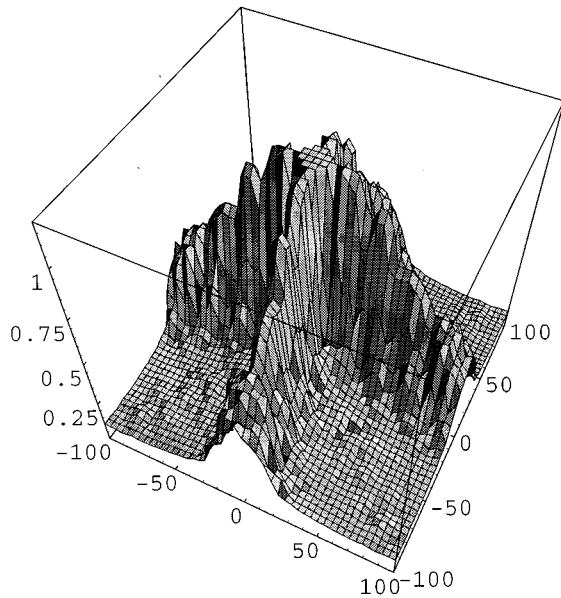


FIG. 6. Same as Fig. 5, but for  $eV = 1.1\Delta_{\max}$ . The features are now rotated  $45^\circ$  relative to Fig. 5.

$\text{Bi}_2\text{Sr}_2\text{CaCu}_2\text{O}_8$  is a layered structure with weakly coupled planes, so we calculate the Green functions for a cylindrical Fermi surface.<sup>2</sup> Figure 5 shows the position-dependent differential conductance as a function of  $x$  and  $y$  (in units of  $\text{\AA}$ ) for the  $d_{x^2-y^2}$  gap  $\Delta_{\mathbf{k}} = \Delta_{\max}\cos(2\phi_{\mathbf{k}})$ .  $\phi_{\mathbf{k}}$  is the angle that the momentum  $\mathbf{k}$  makes with the crystallographic  $a$  axis. The voltage bias is set well below the gap maximum ( $eV = 0.1\Delta_{\max}$ ) so that the quasiparticles are only able to propagate in the directions where  $\Delta_{\mathbf{k}}$  has nodes. A low-pass filter was used to remove the atomic-scale spatial oscillations in  $dI/dV$  characterized by the Fermi wavelength.

In a heuristic sense, gap anisotropy produces an angularly dependent density of states, which can be qualitatively different at different energies. For a  $d_{x^2-y^2}$  gap, at voltages much less than the gap quasiparticles can only travel in the real-space directions roughly parallel to node momenta, yielding “channels” of conductance.<sup>3</sup> At voltages slightly higher than the gap maximum there are more states for momenta near the gap maximum, so the channels would appear rotated by  $45^\circ$ , as shown in Fig. 6. Measurements of gap anisotropy, particularly from angle-resolved photoemission,<sup>18</sup> are of great current interest for distinguishing among various theories of high-temperature superconductivity. Tunneling experiments have an energy resolution better than 1 meV, far superior to angle-resolved photoemission. Again, it is not necessary to rotate the tip assembly since regions of the sample with different orientations could be measured instead.

The signal in this two-protrusion transport experiment is greater than the two-contact or impurity configurations because the interference terms in Eq. (7) are first order (proportional to  $|W|^2$ ). The two-contact experiment relies on a second-order process, proportional to  $|W|^4$ .<sup>3</sup> The impurity transport experiment<sup>2</sup> relies on a process which is first order in tunneling,  $|W|^2$ , and impurity-scattering  $|U|^2$  (the  $U$  is the potential strength), and thus overall is second order.

The primary goal of this paper has been to offer an example of how a two-protrusion STM can explore the characteristics of fluctuating impurity potentials and the local transport properties of a homogeneous sample. The way that a two-protrusion  $dI/dV$  indicates the angular symmetry of an impurity state is similar to the way that a differential cross section of a particle-atom collision indicates the angular symmetry of an atomic state. Measuring gap anisotropy is merely another possible application of the ability to directly and in detail probe small-scale electronic transport.

We acknowledge useful conversations with M.F. Crommie, C.M. Lieber, and A. Yazdani. J.M.B. is supported by The National Research Council.

<sup>1</sup>M.F. Crommie, C.P. Lutz, and D.M. Eigler, *Nature (London)* **363**, 524 (1993). Related phenomena were independently explored on the Au(111) surface [Y. Hasegawa and P. Avouris, *Phys. Rev. Lett.* **71**, 1071 (1993)].  
<sup>2</sup>J.M. Byers, M.E. Flatté, and D.J. Scalapino, *Phys. Rev. Lett.* **71**, 3363 (1993).  
<sup>3</sup>J.M. Byers and M.E. Flatté, *Phys. Rev. Lett.* **75**, 306 (1995).  
<sup>4</sup>Q. Niu, M.C. Chang, and C.K. Shih, *Phys. Rev. B* **51**, 5502 (1995).  
<sup>5</sup>J. Heil, M. Primke, K.U. Würz, and P. Wyder, *Phys. Rev. Lett.* **74**, 146 (1995).  
<sup>6</sup>M.F. Crommie, C.P. Lutz, and D.M. Eigler, *Phys. Rev. B* **48**, 2851 (1993).  
<sup>7</sup>E.J. Heller, M.F. Crommie, C.P. Lutz, and D.M. Eigler, *Nature (London)* **369**, 464 (1994).  
<sup>8</sup>N. Isshiki, K. Kobayashi, and M. Tsukada, *Surf. Sci.* **238**, L439 (1990); *J. Vac. Sci. Technol. B* **9**, 475 (1991).  
<sup>9</sup>M. Crommie (private communication).  
<sup>10</sup>J. Tersoff and D.R. Hamann, *Phys. Rev. B* **31**, 805 (1985).

<sup>11</sup>P.K. Hansma and J. Tersoff, *J. Appl. Phys.* **61**, R1 (1987).  
<sup>12</sup>P. Sautet and C. Joachim, *Chem. Phys. Lett.* **185**, 23 (1991).  
<sup>13</sup>P. Sautet and M.-L. Bocquet, *Surf. Sci. Lett.* **304**, L445 (1994).  
<sup>14</sup>We assume an isotropic electron gas and that the hopping energy from an extended state to the localized state is proportional to their overlap.  
<sup>15</sup>A linear geometry has been assumed for the tip region joining the two protrusions.  
<sup>16</sup>N.E. Bickers, D.J. Scalapino, and S.R. White, *Phys. Rev. Lett.* **62**, 961 (1989); P. Monthoux and D. Pines, *ibid.* **69**, 961 (1992).  
<sup>17</sup>From resistivity measurements the mean free path is 1500  $\text{\AA}$  at 4.2 K in  $\text{YBa}_2\text{Cu}_3\text{O}_7$  [R.P. Robertazzi *et al.*, *Phys. Rev. B* **46**, 8456 (1992)], while from microwave measurements the mean free path is  $1.6\mu$  [D.A. Bonn *et al.*, *Phys. Rev. B* **47**, 11 314 (1993)]. Measurements of similar quality on  $\text{Bi}_2\text{Sr}_2\text{CaCu}_2\text{O}_8$  have not been done, although regions of the surface without imperfections  $500 \times 500 \text{\AA}$  are readily found with STM.  
<sup>18</sup>Z.X. Shen *et al.*, *Science* **267**, 343 (1995).